

Using the Electrostatic Field Effect to Design a New Class of Inhibitors for Cysteine Proteases

Jeffrey L. Conroy, Tanya C. Sanders, and Christopher T. Seto*

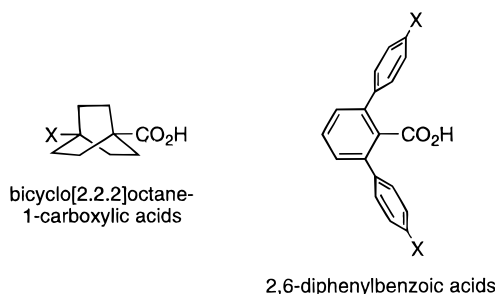
Contribution from the Department of Chemistry, Brown University, Providence, Rhode Island 02912

Received December 4, 1996[⊗]

Abstract: A new class of competitive inhibitors for the cysteine protease papain is described. These inhibitors are based upon a 4-heterocyclohexanone ring and are designed to react with the enzyme active site nucleophile to give a reversibly formed hemithioacetal. The electrophilicity of the ketone in these inhibitors is enhanced by ring strain and by through-space electrostatic repulsion with the heteroatom at the 1-position of the ring. Equilibrium constants for addition of water and 3-mercaptopropionic acid to several 4-heterocyclohexanones were measured by ¹H NMR spectroscopy. These reactions model addition of the active site nucleophile to the corresponding inhibitors. The equilibrium constants give a linear correlation with the field substituent constant *F* for the functional group at the 1-position of the heterocyclohexanone. These equilibrium constants also correlate well with the inhibition constants for the 4-heterocyclohexanone-based inhibitors, which range from 11 to 120 μM. Thus, the model system can be used to predict the potency of structurally related enzyme inhibitors.

Introduction

The Field Effect. The physical-organic literature contains many examples of chemical systems that use through-space electronic interactions to control equilibria or regio- and stereospecificity of organic reactions.^{1,2} Molecules such as 4-substituted bicyclo[2.2.2]octane-1-carboxylic acid have been developed to investigate the Coulombic interaction between a polar substituent and a carboxylic acid.³ The through-space electrostatic interaction between these groups perturbs the p*K*_a of the acid. More recently, Siegel and co-workers examined through-space polar π interactions in *para*-substituted 2,6-diphenylbenzoic acids.⁴ In this system, the substituents alter the polarity of the phenyl rings, which in turn influence the acidity and hydrogen-bonding characteristics of the carboxylic acid. These examples demonstrate that through-space electrostatic interactions can exert a powerful influence on chemical reactions. Despite the importance of these studies, we and others⁴ have noted that through-space interactions are seldom used as a rational design element in bioorganic and medicinal chemistry.⁵ In this paper, we present a physical-organic strategy for designing a new class of inhibitors for cysteine proteases. These inhibitors are based on a 4-heterocyclohexanone nucleus and take advantage of through-space electrostatic repulsion to control the potency of enzyme inhibition.



Other Cysteine Protease Inhibitors. Cysteine proteases are important targets in medicinal chemistry. They have been implicated in diseases such as rheumatoid arthritis,⁶ muscular dystrophy,⁷ and cancer metastasis.⁸ Many types of chemical functionality have served as the central pharmacophore for reversible and irreversible inhibitors of cysteine proteases. Among the reversible inhibitors are aldehydes,⁹ nitriles,¹⁰ α-keto carbonyl compounds,¹¹ and cyclopropanones.¹² Aldehydes and nitriles inhibit proteases by forming a reversible covalent bond between the electrophilic functionality of the inhibitor and the nucleophilic sulfur atom of the active site cysteine residue.¹³

(6) Van Noorden, C. F.; Smith, R. E.; Rasnick, D. *J. Rheumatol.* **1988**, *115*, 1525.

(7) Prous, J. R., Ed. *Drugs Future* **1986**, *11*, 927–943.

(8) (a) Liotta, L. A.; Steeg, P. S.; Stetler-Stevenson, J. G. *Cell* **1991**, *64*, 327. (b) Baricos, W. H.; Zhou, Y.; Mason, R. W.; Barrett, A. *J. Biochem. J.* **1988**, *252*, 301.

(9) (a) Hanzlik, R. P.; Jacober, S. P.; Zygmunt, J. *Biochim. Biophys. Acta* **1991**, *1073*, 33. (b) Cheng, H.; Keitz, P.; Jones, J. B. *J. Org. Chem.* **1994**, *59*, 7671.

(10) Hanzlik, R. P.; Zygmunt, J.; Moon, J. B. *Biochem. Biophys. Acta* **1990**, *1035*, 62.

(11) Hu, L.-Y.; Abeles, R. H. *Arch. Biochem. Biophys.* **1990**, *281*, 271.

(12) Ando, R.; Morinaka, Y.; Tokuyama, H.; Isaka, M.; Nakamura, E. *J. Am. Chem. Soc.* **1993**, *115*, 1174.

(13) (a) Moon, J. B.; Coleman, R. S.; Hanzlik, R. P. *J. Am. Chem. Soc.* **1986**, *108*, 1350. (b) Brisson, J.-R.; Carey, P. R.; Storer, A. C. *J. Biol. Chem.* **1986**, *261*, 9087. (c) Gamcsik, M. P.; Malthous, J. P. G.; Primrose, W. U.; Mackenzie, N. E.; Boyd, A. S. F.; Russell, R. A.; Scott, A. I. *J. Am. Chem. Soc.* **1983**, *105*, 6324. (d) Liang, T.-C.; Abeles, R. H. *Arch. Biochem. Biophys.* **1987**, *252*, 626.

[⊗] Abstract published in *Advance ACS Abstracts*, May 1, 1997.

(1) (a) Winstein, S.; Shatavsky, M.; Norton, C.; Woodward, R. B. *J. Am. Chem. Soc.* **1955**, *77*, 4183. (b) Winstein, S.; Shatavsky, M. *J. Am. Chem. Soc.* **1956**, *78*, 592. (c) For a recent review, see: Bowden, K.; Grubbs, E. *J. Chem. Soc. Rev.* **1996**, *25*, 171.

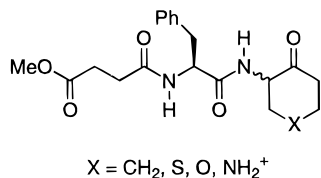
(2) Lowry, T. H.; Richardson, K. S. *Mechanism and Theory in Organic Chemistry*, 3rd ed.; Harper and Row: New York, 1987.

(3) (a) Roberts, J. D.; Moreland, W. T., Jr. *J. Am. Chem. Soc.* **1953**, *75*, 2167. (b) Holtz, H. D.; Stock, L. M. *J. Am. Chem. Soc.* **1964**, *86*, 5188.

(4) Chen, C.-T.; Siegel, J. S. *J. Am. Chem. Soc.* **1994**, *116*, 5959.

(5) (a) For an example taken from synthetic organic chemistry, see: Boeckman, R. K., Jr.; Connell, B. T. *J. Am. Chem. Soc.* **1995**, *117*, 12368.

(b) For a discussion of field and resonance effects in benzoxazinone inhibitors of human leukocyte elastase, see: Krantz, A.; Spencer, R. W.; Tam, T. F.; Liak, T. J.; Copp, L. J.; Thomas, E. M.; Rafferty, S. P. *J. Med. Chem.* **1990**, *33*, 464.

Chart 1. Structures of Cysteine Protease Inhibitors

This mechanism is also likely to be operative in the α -keto carbonyl¹¹ and cyclopropenone inhibitors.

Design of Inhibitors. Chart 1 shows the structures of 4-heterocyclohexanone-based inhibitors for the cysteine protease papain. These inhibitors consist of a 4-heterocyclohexanone core that is appended with an *N*-(methoxysuccinyl)phenylalanine side chain. We have chosen papain for our initial studies because its structure and mechanism have been thoroughly characterized. In addition, it provides a good model for evaluating the design of new inhibitors and for comparing them to previously reported compounds. The inhibitors include a phenylalanine residue because papain has a high specificity for this amino acid at the P2 position.¹⁴ The methoxysuccinyl group was attached in order to increase solubility of the compounds in aqueous solution.

The inhibitors incorporate an electrophilic ketone moiety that is designed to give a reversibly formed hemithioketal with the enzyme active site nucleophile, in analogy with previously reported inhibitors. Compounds based upon unactivated ketones are not electrophilic enough to react with the active site cysteine nucleophile.¹⁵ However, the carbonyl groups in 4-heterocyclohexanones are more electrophilic than standard ketones. Two factors increase their reactivity. First, there is an unfavorable dipole–dipole repulsion between the carbonyl and the heteroatom at the 1-position of the ring.^{16–18} This interaction destabilizes the ketone, but is dissipated by addition of nucleophiles. Second, ring strain enhances the reactivity of 4-heterocyclohexanones. The cyclic compounds are more strained than their acyclic counterparts, and this strain is relieved by nucleophilic addition to the carbonyl to give a tetrahedral center.^{18,19} Variations in the bond angles and bond lengths associated with the heteroatom will modulate this effect.²⁰

An alternate method for increasing the electrophilicity of ketones is to add electron-withdrawing substituents to them. This strategy, which relies on through-bond inductive effects, has been implemented in the synthesis of potent trifluoromethyl ketone inhibitors of serine proteases.²¹ However, these compounds have been found to be poor reversible inhibitors of cysteine proteases.²²

We have synthesized a series of inhibitors that incorporate increasingly electronegative functional groups at the 1-position

(14) (a) Hanzlik, R. P.; Jacober, S. P.; Zygmunt, J. *Biochim. Biophys. Acta* **1991**, *1073*, 33. (b) Berti, P. J.; Faerman, C. H.; Storer, A. C. *Biochemistry* **1991**, *30*, 1394.

(15) Bendall, M. R.; Cartwright, I. L.; Clart, P. I.; Lowe, G.; Nurse, D. *Eur. J. Biochem.* **1977**, *79*, 201.

(16) Geneste, P.; Durand, R.; Hugon, I.; Reminiac, C. *J. Org. Chem.* **1979**, *44*, 1971.

(17) Das, G.; Thornton, E. R. *J. Am. Chem. Soc.* **1993**, *115*, 1302.

(18) Burkey, T. J.; Fahey, R. C. *J. Org. Chem.* **1985**, *50*, 1304.

(19) (a) Allinger, N. L.; Tribble, M. T.; Miller, M. A. *Tetrahedron* **1972**, *28*, 1173. (b) Gung, B. W.; Wolf, M. A.; Mareska, D. A.; Karipides, A. J. *Org. Chem.* **1994**, *59*, 4899.

(20) Transannular anomeric interactions have been used previously to explain reaction rates and axial selectivities for addition of nucleophiles to 4-heterocyclohexanones. It is possible that these types of interactions also stabilize the hemithioketal that results from nucleophilic addition of a thiol to these ketones. (a) Cieplak, A. S. *J. Am. Chem. Soc.* **1981**, *103*, 4540. (b) Cieplak, A. S. *J. Am. Chem. Soc.* **1989**, *111*, 8447 and references therein.

(21) (a) Imperiali, B.; Abeles, R. H. *Biochemistry* **1986**, *25*, 3760. (b) Brady, K.; Abeles, R. H. *Biochemistry* **1990**, *29*, 7608. (c) Govardhan, C. P.; Abeles, R. H. *Arch. Biochem. Biophys.* **1990**, *280*, 137.

Table 1. Equilibrium Constants for Addition of Water and Thiol to Selected Ketones^a

X	$K_{\text{H}_2\text{O}}$ (M ⁻¹)	K_{RSH} (M ⁻¹)	$K_{\text{RSH,app}}$ (M ⁻¹)
CH ₂	8.1×10^{-4}	0.22	0.21
S	9.0×10^{-3}	1.5	0.99
O	8.0×10^{-3}	1.8	1.3
NH ₂ ⁺	0.18	27.6	2.7
SO	0.068	11.7	2.5
SO ₂	0.30	60.2	3.5
Other Ketones			
CH ₃ COCH ₃ ^b	2.3×10^{-5}	0.0052	0.0052
CH ₃ COCO ₂ H ^b	0.031	58	22
CH ₃ COCO ₂ CH ₃ ^b	0.045	71	20

^a RSH = HO₂CCH₂CH₂SH. ^b Data taken from reference 23.

of the heterocyclohexanone ring. These compounds have allowed us to examine the relationship between the electronic characteristics of the X group (Chart 1) and the potency of the inhibitor. Electronegative X groups are expected to destabilize the ketone via through-space electrostatic repulsion, thereby shifting the ketone–hemithioketal equilibrium in favor of the hemithioketal and resulting in more potent inhibition.

The compounds reported in this paper are first-generation inhibitors that interact only with the S subsites of the enzyme active site. However, the 4-heterocyclohexanone nucleus can be derivatized on both sides of the electrophilic carbonyl to yield inhibitors that make contacts with both the S and S' subsites. This is in contrast to aldehyde- and nitrile-based inhibitors that are limited to interactions with only half of the active site.

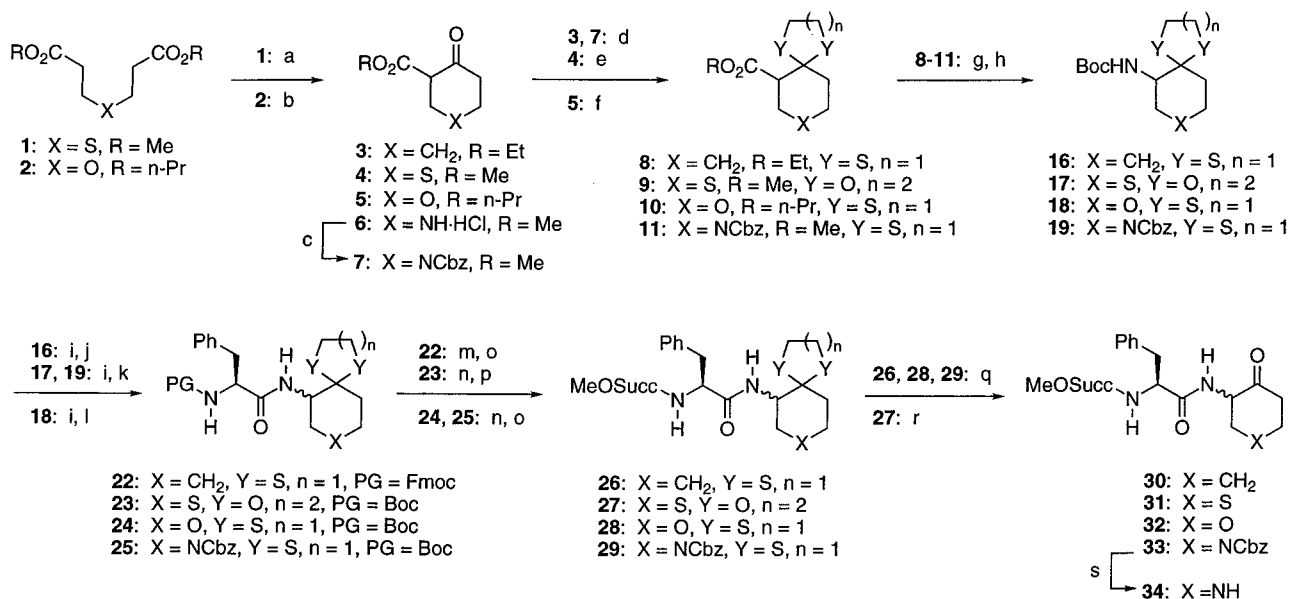
Results

Model System. Before we undertook the multistep synthesis of our cysteine protease inhibitors, we first wanted to investigate the degree to which the heteroatom influences the reactivity of the ketone in these compounds. We have thus measured the equilibrium constants for addition of water and thiol nucleophiles to simple 4-heterocyclohexanones. These nucleophilic additions serve as a model for reaction of the enzyme active site nucleophile with the inhibitors.

Table 1 shows equilibrium constants for addition of water and 3-mercaptopropionic acid to a variety of ketones. The equilibrium constants were determined using ¹H NMR spectroscopy according to the procedure of Burkey and Fahey.^{18,23} Figure 1 shows NMR spectra of tetrahydropyran-4-one as an example of how these measurements were made. The bottom spectrum, taken in acetone-*d*₆, shows resonances that correspond to tetrahydropyranone. The middle spectrum, taken in D₂O, shows resonances for the both the ketone (a and b) and the hydrate (c and d). These two species are in slow exchange on the NMR time scale. Integration of the resonances can be used to determine the hydration equilibrium constant. The top spectrum shows a mixture of tetrahydropyranone and 3-mercaptopropionic acid in D₂O. We observe resonances for ketone, hydrate, hemithioketal (e–h), and free thiol (i and j). Equilibrium constants for several of the ketones listed in Table 1 have been measured previously under different reaction conditions.^{18,24} Our equilibrium constants are in reasonable agreement with the

(22) (a) Smith, R. A.; Copp, L. J.; Donnelly, S. L.; Spencer, R. W.; Krantz, A. *Biochemistry* **1988**, *27*, 6568. (b) Peptide monofluoromethyl ketones have been shown to be selective irreversible inhibitors of cysteine proteases: Rasnick, D. *Anal. Biochem.* **1985**, *149*, 461. (c) Rauber, P.; Angliker, H.; Walker, B.; Shaw, E. *Biochem. J.* **1986**, *239*, 633.

(23) Burkey, T. J.; Fahey, R. C. *J. Am. Chem. Soc.* **1983**, *105*, 868.

Scheme 1^a

^a (a) NaH, catalytic MeOH, 81%; (b) LDA, THF, -78 °C, 31%; (c) CbzCl, TEA, 95%; (d) ethanedithiol, TsOH, 94% from **3**, 74% from **7**; (e) 1,3-propanediol, TsOH, 77%; (f) ethanedithiol, BF₃·Et₂O, 43%; (g) NaOH, MeOH; (h) diphenylphosphoryl azide, benzene, followed by *t*-BuOK, THF, 60% from **8**, 37% from **9**, 44% from **10**, 71% from **11** (two step yields); (i) TFA, CH₂Cl₂; (j) FmocPhe-F, DIEA, 92% (two steps); (k) BocPhe-OH, EDC, HOBT, 84% from **17**, 81% from **19** (two step yields); (l) BocPhe-F, DIEA, 61% (two steps); (m) N(CH₂CH₂NH₂)₃, CH₂Cl₂; (n) TFA, CH₂Cl₂; (o) monomethyl succinate, EDC, HOBT, 70% from **22**, 70% from **24**, 89% from **25** (two step yields); (p) methyl(*N*-hydroxysuccinimidyl) succinate, DIEA, 77% (two steps); (q) NBS, H₂O, 80% from **26**, 66% from **28**, 68% from **29**; (r) acetone, TsOH, 79%; (s) H₂, 5% Pd/C, 79%.

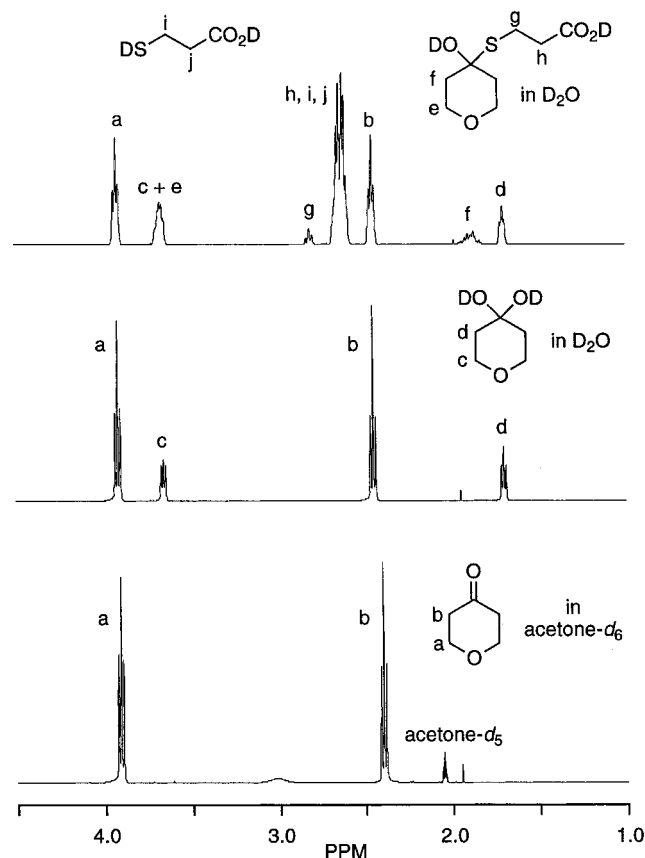


Figure 1. ¹H NMR spectra of the ketone, hydrate, and hemithioketal of tetrahydropyranone. The bottom spectrum shows the ketone in acetone-*d*₆ solution. The middle spectrum shows a mixture of ketone and hydrate in D₂O solution. The top spectrum shows a mixture of ketone, hydrate, hemithioketal, and free thiol in D₂O solution.

previously reported values. Equilibrium constants for acetone, pyruvic acid, and methyl pyruvate are taken from the literature.²³

The hydration equilibrium constant for cyclohexanone is 35 times greater than that of acetone. In cyclohexanone, ring strain

destabilizes the ketone and shifts the equilibrium by 2.1 kcal/mol in favor of hydrate when compared to acetone. Substituting electronegative functionality at the 4-position of the cyclohexanone ring leads to further destabilization of the ketone as a result of through-space electrostatic repulsion. For example, in the sulfone-containing molecule, the equilibrium is shifted by an additional 3.5 kcal/mol in favor of the hydrate. These results demonstrate that the electrostatic field effect, in combination with ring strain, can have a significant influence on the stability of hydrates. Similar trends are observed for the formation of hemithioketals.

The reaction between an enzyme and an inhibitor occurs in an aqueous environment. We must therefore consider that reaction between papain and the 4-heterocyclohexanone-based inhibitors will occur in competition with reaction between the inhibitor and water. This competition will lower the effective concentration of the inhibitor. We have calculated an *apparent* equilibrium constant for addition of thiol to ketone ($K_{\text{RSH,app}}$), first described by Jencks,²⁵ that accounts for the fact that the inhibitor will be present as a mixture of both ketone and hydrate in aqueous solution.

$$K_{\text{RSH,app}} = \frac{[\text{hemithioketal}]}{[\text{ketone} + \text{hydrate}][\text{thiol}]} = \frac{K_{\text{RSH}}}{(1 + K_{\text{H}_2\text{O}}[\text{H}_2\text{O}])} \quad (1)$$

For molecules such as acetone that form a minimal amount of hydrate, the $K_{\text{RSH,app}}$ value is approximately equal to K_{RSH} . However, if a ketone forms a significant amount of hydrate, then $K_{\text{RSH,app}}$ is less than K_{RSH} . If the ketone, but not the hydrate form of these compounds, is the active inhibitory species, we would expect a correlation between the $K_{\text{RSH,app}}$ value of the parent ketone and the potency of the corresponding inhibitor.

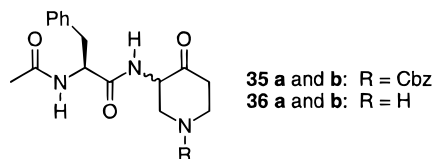
Synthesis of Inhibitors. We have developed a generalized strategy for the synthesis of our papain inhibitors (Scheme 1). This strategy allows us to perform similar reactions in the

(24) (a) Wiberg, K. B.; Morgan, K. M.; Maltz, H. *J. Am. Chem. Soc.* **1994**, *116*, 11067. (b) Van Luppen, J. J.; Lepoivre, J. A.; Dommissée, R. A.; Alderweireldt, F. C. *Org. Magn. Reson.* **1979**, *12*, 399.

(25) Sanders, E. G.; Jencks, W. P. *J. Am. Chem. Soc.* **1968**, *90*, 6154.

preparation of each of the four target compounds. Dieckmann condensation of diesters **1** and **2** gives keto esters **4** and **5**. Compounds **3** and **6** are commercially available. The yield for cyclization of **2** is only 31%, presumably because of competing β -elimination. However, this represents a significant improvement over the previously reported synthesis of methyl tetrahydropyran-4-one-3-carboxylate, which proceeded in 8% yield.²⁶ The ketones in compounds **3**, **5**, and **7** are protected as thioketals. Since the oxidative conditions that are used for removal of this protecting group are not compatible with thioethers, compound **4** is protected as an oxygen ketal. The esters are hydrolyzed and the resulting carboxylic acids are treated with diphenylphosphoryl azide.²⁷ Curtius rearrangement followed by trapping of the isocyanates with *t*-BuOK gives carbamates **16–19**. The Boc protecting groups are removed with trifluoroacetic acid, and the resulting amines are coupled with an N-protected phenylalanine derivative.²⁸ After removing the phenylalanine protecting groups, the free amines are coupled to monomethyl succinate to give compounds **26–29**. The thioether protecting groups in compounds **26**, **28**, and **29** are removed by treatment with *N*-bromosuccinimide,²⁹ and the diastereomers of inhibitors **30** and **32** are separated by HPLC. The Cbz protecting group in compound **33** is removed by catalytic hydrogenation to give inhibitor **34**, which is evaluated as a mixture of diastereomers. The diastereomers of **27** can be separated by flash chromatography, and each are then treated with acetone and *p*-toluenesulfonic acid to give the separate diastereomers of inhibitor **31**.

Racemization of Inhibitors. Papain is assayed in 100 mM phosphate buffer at pH 6.5. These conditions may catalyze the enolization of the ketone in our inhibitors and thus lead to their racemization. We have monitored this reaction using HPLC or ¹H NMR spectroscopy. The cyclohexanone-based inhibitor **30** was very stable under the assay conditions, showing less than 5% racemization after 24 h. Tetrahydropyranone **32** was somewhat less stable, with a half-time for racemization of 5.25 h. However, this reaction is slow enough so that over the time period of a typical enzyme assay, the compound racemizes less than 1%. We were unable to separate the diastereomers of piperidone inhibitor **34** or its precursor **33** by standard chromatographic techniques. However, the diastereomers of compound **35**, which has an acetyl group on its N-terminus rather than a methoxysuccinyl group, were readily separated by HPLC. We therefore chose to study racemization of compound **36** by ¹H NMR spectroscopy. Over the course of the 10 min required



to prepare the sample and acquire the spectrum, this compound was completely racemized. Therefore, we measured the inhibition constant for compound **34** as a mixture of diastereomers. We have not examined racemization of the tetrahydrothiopyranone-based inhibitor **31**, but observed reactivity trends and chemical intuition both suggest that it should have a racemization rate that falls between that of compounds **30** and **32**.

Inhibition Studies. The 4-heterocyclohexanone-based inhibitors **30–32** and **34** are all reversible competitive inhibitors

(26) Dowd, P.; Choi, S.-C. *Tetrahedron* **1991**, *47*, 4847.

(27) Shioiri, T.; Ninomiya, K.; Yamada, S. *J. Am. Chem. Soc.* **1972**, *94*, 6203.

(28) (a) Carpino, L. A.; Sadat-Aalae, D.; Chao, H. G.; DeSelms, R. H. *J. Am. Chem. Soc.* **1990**, *112*, 9651. (b) Carpino, L. A.; Mansour, E. M. E.; Sadat-Aalae, D. *J. Org. Chem.* **1991**, *56*, 2611.

(29) Corey, E. J.; Erickson, B. W. *J. Org. Chem.* **1971**, *36*, 3553.

Table 2. Inhibition of Papain by 4-Heterocyclohexanone-Based Inhibitors

X	K_i (μ M)	
	more-potent diastereomer	less-potent diastereomer
CH ₂	78	3200
S	26	2400
O	11	3300
NH ₂ ⁺	121 ^a	
Other Ketone-Based Inhibitors		
AcPhe-NHCH ₂ COMe		1550 ^b
ZPhe-NHCH ₂ COCO ₂ H		7 ^c
ZPhe-NHCH ₂ COCO ₂ Me		1 ^c

^a Assayed as a mixture of diastereomers. This compound racemizes under the assay conditions. ^b Data from ref 15. ^c Data from ref 11.

of papain (Table 2).³⁰ The enzyme shows a clear preference for one diastereomer of each inhibitor, although we have not determined the absolute configuration of the tighter binding diastereomer. Data for the acetone-, pyruvic acid-, and methyl pyruvate-based inhibitors are included in Table 2 for comparison. Although these three reference compounds do not have a methoxysuccinyl group on their N-terminus, our previous work has demonstrated that inhibitors with *N*-acetyl or *N*-Cbz blocking groups have inhibition constants that are within a factor of two of the *N*-methoxysuccinyl compounds.

The cyclohexanone-based inhibitor (X = CH₂) is 20 times more potent than the noncyclic acetone-based inhibitor. This is a reflection of the ring strain in cyclohexanone that destabilizes the ketone relative to the hemithioacetal that is formed by reaction of the inhibitor with the active site nucleophile. Substituting electronegative functionality into the ring (X = S, O) leads to even better inhibitors. This trend in inhibition constants mirrors the differences that we observe for reaction of the parent ketones with water and thiol nucleophiles. The only compound that does not fit the trend is the piperidone-based inhibitor **34**. This compound is protonated under the assay conditions (pH 6.5), and its low potency is likely caused by the unfavorability of placing this positive charge into the enzyme active site.⁹

Discussion

Linear Free-Energy Relationship. We observe a correlation between the reactivity of 4-heterocyclohexanones and the electronic properties of the heteroatom in these molecules. This correlation requires an appropriate description of the magnitude of the through-space electrostatic repulsion between the heteroatom and the ketone. Swain and Lupton³¹ have constructed a modified Hammett equation (eq 2) in which they describe the electronic characteristics of substituents in terms of two parameters; a field substituent constant *F*, and a resonance substituent constant *R*.

$$\log(K_x/K_H) = \rho(fF + rR) \quad (2)$$

The terms *f* and *r* are empirical weighing factors that are specific for the particular reaction and set of reaction conditions,

(30) Enzyme assays were performed according to the procedures of ref 11. None of these compounds showed evidence of slow-binding inhibition. Lineweaver–Burk plots are available in the Supporting Information.

(31) (a) Swain, C. G.; Lupton, E. C., Jr. *J. Am. Chem. Soc.* **1968**, *90*, 4328. (b) Swain, C. G.; Unger, S. H.; Rosenquist, N. R.; Swain, M. S. *J. Am. Chem. Soc.* **1983**, *105*, 492.

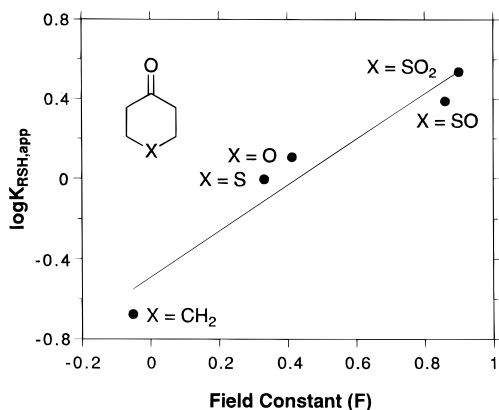


Figure 2. Correlation between the logarithm of the apparent equilibrium constant for addition of thiol to 4-heterocyclohexanones and the field substituent constant F ($\log K_{\text{RSH,app}} = 1.1F - 0.5$; correlation coefficient = 0.97).

while the F and R parameters are independent of the reaction. If the major interaction between the heteroatom and ketone is electrostatic, then the field substituent constant F should provide a good measure of this interaction.

The chemical systems that are used to define field substituent constants are designed so that the substituents are attached to the parent molecules through a single bond.³¹ However, in 4-heterocyclohexanones the heteroatom is attached by two bonds. We have thus approximated the functionality at the 1-position of heterocyclohexan-4-ones by using the field constant for the substituents $-\text{CH}_3$, $-\text{SCH}_3$, $-\text{OCH}_3$, $-\text{SOCH}_3$, and $-\text{SO}_2\text{CH}_3$. Protonated piperidone has been omitted from our analysis because the F value for the corresponding substituent, $-\text{NH}_2\text{CH}_3^+$, has not been reported.

Figure 2 shows that there is a good correlation between the logarithm of the apparent equilibrium constants for addition of thiol to 4-heterocyclohexanones ($\log K_{\text{RSH,app}}$) and the field substituent constants.³² This correlation confirms that the interaction between the heteroatom and the ketone in 4-heterocyclohexanones is best described as a through-space electrostatic repulsion. Resonance effects, differences in ring strain, and transannular anomeric effects²⁰ have a relatively minor influence on the equilibria of the reversible addition of water and thiol nucleophiles to these ketones. The slope of the line in Figure 2 is 1.1. A similar plot for dissociation of 4-substituted benzoic acids has a slope of 0.49.³¹ Comparison of these values suggests that addition of thiols to 4-heterocyclohexanones responds two times more strongly to the *field component* of the electronic effects exerted by substituents. The larger slope for the addition reaction is reasonable because the substituent and reaction center are closer together than they are in 4-substituted benzoic acids.

Correlation between Ketone Reactivity and Enzyme Inhibition. We have designed our cysteine protease inhibitors on the basis of the supposition that inhibitor potency is controlled by the stability of the hemithioketal that results from addition of the active site nucleophile to the inhibitor, although we have not proved the existence of this hemithioketal through structural studies. If this supposition is correct, we should observe a correlation between inhibition constants and the equilibrium constants for addition of thiol to the parent ketones. Because enzyme inhibition takes place in aqueous solvent, the most appropriate comparison is between inhibition constants and $K_{\text{RSH,app}}$ values.³³

(32) A good correlation also exists between $\log K_{\text{RSH}}$ and F and between $\log K_{\text{H}_2\text{O}}$ and F . However, there is a poor correlation between $\log K_{\text{RSH,app}}$ and the resonance substituent constant R (correlation coefficient = 0.41).

(33) For a similar analysis involving inhibitors of cathepsin B, see: ref 22a.

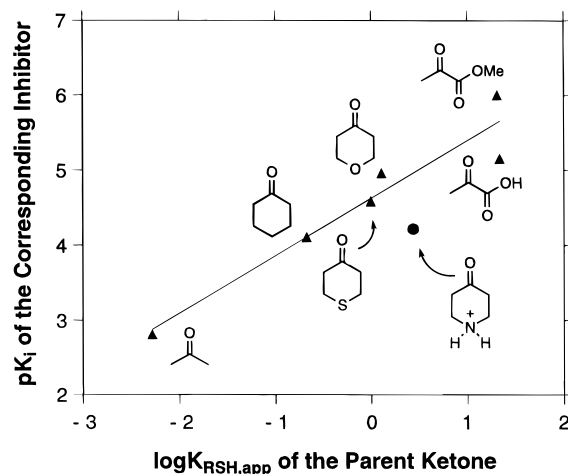


Figure 3. Correlation between inhibition constant (pK_i) of the ketone-based inhibitors and the logarithm of the apparent equilibrium constant for addition of thiol to the parent ketones ($pK_i = 0.8 \log K_{\text{RSH,app}} + 4.6$; correlation coefficient = 0.96).

The correlation shown in Figure 3 demonstrates that addition of 3-mercaptopropionic acid to simple ketones in aqueous solution is an appropriate model for addition of the enzyme active site cysteine residue to the corresponding ketone-based inhibitors. The apparent equilibrium constant for the model reaction provides a good prediction of inhibitor potency for this structurally homologous series of compounds. The plot of pK_i vs $\log K_{\text{RSH,app}}$ has a slope of 0.8. This slope, which is less than unity, indicates that the enzymatic addition reaction responds less efficiently to the electrophilicity of the ketone than does the model system. The difference in reactivity is likely caused by the differences in steric, electronic, solvation, and orientational requirements of the enzymatic reaction compared to the reaction in solution.

We have omitted the piperidone-based inhibitor **34** from the linear regression in Figure 3 because the positive charge on this molecule perturbs its reactivity with the enzyme. As expected, this inhibitor does not fit well into a correlation that is based simply upon electrophilicity of the ketone in these molecules.

Conclusions. The results presented in this paper demonstrate that through-space electrostatic interactions can be useful and predictable design elements for construction of bioactive molecules. The physical-organic correlations point the way toward synthesis of more potent inhibitors. This goal can be achieved by choosing functionality that further increase the electrostatic repulsion between the heteroatom and the ketone in 4-heterocyclohexanones, such as a sulfoxide or sulfone. In addition, potency and specificity can be increased by functionalizing both the 3- and 5-positions of the heterocyclohexanone ring so that we extend noncovalent interactions of the inhibitor into the leaving group subsites. Future studies will be aimed toward proving formation of the hemithioketal intermediate using ^{13}C NMR spectroscopy in conjunction with an inhibitor that is labeled with ^{13}C at the ketone carbon.

Experimental Section

General Methods. NMR spectra were recorded on Bruker WM-250 or AM-400 instruments. Spectra were calibrated using TMS ($\delta = 0.00$ ppm) for ^1H NMR and CDCl_3 ($\delta = 77.0$) for ^{13}C NMR. IR spectra were recorded on a Perkin-Elmer 1700 series FT-IR spectrometer. Mass spectra were recorded on a Kratos MS 80 under electron impact (EI), chemical ionization (CI), or fast-atom bombardment (FAB) conditions. HPLC analyses were performed on a Rainin HPLC system with Rainin Microsorb silica or C18 columns and UV detection. Semipreparative HPLC was performed on the same system using a semipreparative column (21.4×250 mm).

Reactions were conducted under an atmosphere of dry nitrogen in oven-dried glassware. Anhydrous procedures were conducted using standard syringe and cannula transfer techniques. THF and toluene were distilled from sodium and benzophenone. Methylene chloride was distilled from CaH₂. Other solvents were of reagent grade and were stored over 4 Å molecular sieves. All other reagents were used as received. Organic solutions were dried with MgSO₄ unless otherwise noted. Solvent removal was performed by rotary evaporation at water aspirator pressure.

Experimental details of the synthesis of inhibitors **30**, **31**, and **34** are available in the Supporting Information.

Di-*n*-propyl 4-Oxa-1,7-heptanedioate 2. A solution of 3,3'-oxydipropionitrile (18.9 g, 152 mmol) and *p*-toluenesulfonic acid (*p*-TsOH) monohydrate (115.8 g, 608 mmol) in *n*-propanol (200 mL) was refluxed for 24 h. The solution was cooled and concentrated to approximately 150 mL. The resulting solution was partitioned between 350 mL of water and 350 mL of hexanes. The organic layer was separated and washed with saturated NaHCO₃ (200 mL), water (300 mL), and brine (150 mL). The solution was dried, filtered, and concentrated, and the crude material was purified by flash chromatography (1:3 EtOAc/hexanes) to yield **2** (21.2 g, 57%) as a colorless liquid. The product can also be purified by vacuum distillation (bp 158 °C, 6 mm) in somewhat lower yields (45%): *R_f* 0.66 (1:1 EtOAc/hexanes); ¹H NMR (400 MHz, CDCl₃) δ 0.94 (t, *J* = 7.4 Hz, 3H), 1.66 (dt, *J* = 7.0, 7.1 Hz, 2H), 2.57 (t, *J* = 6.1 Hz, 2H), 3.73 (t, *J* = 6.4 Hz, 2H), 4.04 (t, *J* = 6.7 Hz, 2H); ¹³C NMR (100 MHz, CDCl₃) δ 10.3, 21.9, 35.0, 66.1, 66.4, 171.5; HRMS-FAB calcd for C₁₂H₂₂O₅ 246.1467, found 246.1467.

***n*-Propyl Tetrahydropyran-4-one-3-carboxylate 5.** To a solution of diisopropylamine (4.65 g, 45.9 mmol) in THF (50 mL) at -78 °C was added *n*-butyllithium (4.38 mL of 10.0 M in hexanes). This solution was added via cannula to a solution of **2** (5.14 g, 20.9 mmol) in THF (300 mL) at -78 °C. The solution was stirred at -78 °C for 15 min, and then the reaction was quenched by the addition of 25 mL of H₂O. The solution was partitioned between 200 mL of 1 N HCl and 200 mL of hexanes. The resulting aqueous layer was extracted with EtOAc (150 mL), and the combined organic layers were washed with brine (300 mL). The solution was dried, filtered, and concentrated, and the crude material purified by flash chromatography (1:4 Et₂O/hexanes) to yield **5** (1.19 g, 31%) as a mixture of keto and enol tautomers: *R_f* = 0.54 (1:1 Et₂O/hexanes); ¹H NMR (400 MHz, CDCl₃) δ 0.95 (t, *J* = 6.3 Hz, 3H), 1.27–1.31 (m), 1.61–1.75 (m, 2H), 2.37–2.41 (m, 3H), 2.52–2.59 (m), 2.66–2.73 (m), 3.46–3.50 (m), 3.71–3.75 (m), 3.85 (t, *J* = 5.7 Hz, 2H), 3.98–4.10 (m), 4.12 (t, *J* = 6.6 Hz, 2H), 4.16–4.25 (m), 4.28 (t, *J* = 1.7 Hz, 2H), 11.85 (s, 1H); ¹³C NMR (100 MHz, CDCl₃) δ 10.2, 21.9, 28.6, 41.8, 57.8, 63.9, 65.8, 66.3, 67.0, 68.1, 69.6, 97.4, 127.8, 129.7, 168.7, 170.1, 201.4; HRMS-EI (M⁺) calcd for C₉H₁₄O₄ 186.0892, found 186.0894.

Tetrahydropyranone Thioketal 10. To a solution of **5** (1.26 g, 6.8 mmol) and 1,2-ethanedithiol (1.28 g, 13.6 mmol) in CH₂Cl₂ (20 mL) cooled in an ice bath was added BF₃·Et₂O (1.04 mL, 8.5 mmol). The solution was stirred at 0 °C for 4 h, and then it was washed with 10% aqueous NaOH solution, water, and brine (20 mL). The organic layer was dried, and concentrated, and the crude material was purified by flash chromatography (2:3 EtOAc/hexanes) to yield **10** (0.77 g, 43%) as a colorless oil: ¹H NMR (400 MHz, CDCl₃) δ 0.96 (t, *J* = 7.4 Hz, 3H), 1.63–1.73 (m, 2H), 1.93 (dm, *J* = 13.7 Hz, 1H), 2.84–2.88 (m, 1H), 2.91–2.92 (m, 1H), 3.24–3.32 (m, 4H), 3.64–3.69 (m, 1H), 3.90–3.93 (m, 2H), 4.08–4.14 (m, 3H); ¹³C NMR (100 MHz, CDCl₃) δ 10.4, 21.9, 38.3, 39.1, 40.0, 54.8, 65.7, 67.8, 69.5, 171.0; HRMS-EI (M⁺) calcd for C₁₁H₁₈O₃S₂ 262.0697, found 262.0707.

Tetrahydropyranone Carboxylic Acid 14. To a solution of **10** (0.41 g, 1.58 mmol) in MeOH (10 mL) was added 1 N NaOH (10 mL). The solution was stirred at 30 °C for 50 h. The solution was then cooled and diluted with 0.2 N NaOH (10 mL). The solution was washed with 1:1 EtOAc/hexanes (10 mL), and the aqueous layer was separated and acidified with 1 N HCl. The acidic aqueous solution was extracted with EtOAc (2 × 40 mL). These organic extracts were washed with brine (50 mL), dried, and concentrated. The resulting solid was recrystallized from EtOAc/hexanes to yield **14** (0.22 g, 68%) as a white solid: ¹H NMR (400 MHz, CDCl₃) δ 1.98 (d, *J* = 13.8 Hz, 1H), 2.76 (m, 1H), 2.99 (t, *J* = 3.3 Hz, 1H), 3.29–3.35 (m, 4H), 3.68–3.74 (m, 1H), 3.88 (t, *J* = 4.3 Hz, 1H), 3.93 (t, *J* = 4.2 Hz, 1H), 3.99

(dd, *J* = 3.4, 12.2 Hz, 1H), 4.12 (dd, *J* = 3.4, 11.8 Hz, 1H); ¹³C NMR (100 MHz, CDCl₃) δ 38.5, 39.2, 40.3, 54.2, 65.5, 67.8, 69.2; HRMS-EI (M⁺) calcd for C₈H₁₂O₃S₂ 220.0228, found 220.0224.

Tetrahydropyranone Carbamate 18. A solution of **14** (0.22 g, 1.0 mmol), *N,N*-diisopropylethylamine (DIEA, 1.9 g, 1.50 mmol), and diphenylphosphoryl azide (DPPA, 0.28 g, 1.0 mmol) in benzene (10 mL) was refluxed overnight. Aliquots of the reaction mixture were monitored for disappearance of the acyl azide peak at 2168 cm⁻¹ and appearance of the isocyanate peak at 2245 cm⁻¹ by FT-IR. After the Curtius rearrangement was judged complete by IR, the solution was cooled in an ice bath and slowly added to an ice-cold solution of potassium *tert*-butoxide (0.34 g, 3.0 mmol) in THF (10 mL). The reaction was stirred for 15 min and then partitioned between 15 mL of 1 N HCl and 15 mL of EtOAc. The organic layer was separated and washed with 1 N NaOH and brine (15 mL). The solution was dried, filtered, and concentrated, and the crude material was purified by flash chromatography (1:4 EtOAc/hexanes) to yield **18** (0.19 g, 65%) as a white solid: ¹H NMR (400 MHz, CDCl₃) δ 1.45 (s, 9H), 2.21 (t, *J* = 4.5 Hz, 2H), 3.26–3.35 (m, 4H), 3.61–3.64 (m, 1H), 3.79–3.82 (m, 1H), 3.89–3.99 (m, 2H), 5.04 (brd, *J* = 7.7 Hz, 1H); ¹³C NMR (100 MHz, CDCl₃) δ 27.5, 37.7, 37.9, 40.9, 54.2, 66.1, 70.0, 78.1, 154.4; HRMS-EI (M⁺) calcd for C₁₂H₂₁NO₃S₂ 291.0963, found 291.0959.

Aminotetrahydropyranone-Trifluoroacetic Acid Salt 21. Trifluoroacetic acid (TFA, 3.0 mL) was added to a solution of **18** (0.18 g, 0.62 mmol) in CH₂Cl₂ (10 mL) that was cooled in an ice bath. The reaction was stirred at 0 °C for 1 h, concentrated, redissolved in CH₂Cl₂, and then concentrated again to remove excess TFA. The crude oil was then triturated with ether to yield **21** (0.18 g, 95%) as a white solid: ¹H NMR (400 MHz, CDCl₃) δ 2.14 (dt, *J* = 14.3, 5.6 Hz, 1H), 2.44 (dt, *J* = 14.1, 5.0 Hz, 1H), 3.32–3.47 (m, 5H), 3.70–3.76 (m, 3H), 4.04 (dd, *J* = 12.2, 3.0 Hz, 1H); ¹³C NMR (100 MHz, CDCl₃) δ 39.9, 40.1, 41.1, 56.7, 68.1, 68.5, 68.6, 118.2 (q), 162.9 (q); HRMS-EI (M⁺) calcd for C₇H₁₃NOS₂ 191.0439, found 191.0437.

Phenylalanyl tetrahydropyranone 24. To a solution of **21** (250 mg, 0.82 mmol) and DIEA (529 mg, 4.1 mmol) in CH₂Cl₂ (10 mL) was added solid *N*-Boc-phenylalanyl fluoride²⁸ (240 mg, 0.90 mmol). The solution was stirred for 1 h and then washed with 1 N HCl, saturated NaHCO₃, and brine (10 mL). The solution was dried over Na₂CO₃ and concentrated, and the crude material was purified by flash chromatography (2:3 EtOAc/hexanes) to yield a mixture of diastereomers of **24** (218 mg, 61%) as a white solid: ¹H NMR (400 MHz, CDCl₃) δ 1.31 (s, 9H), 1.34 (s, 9H), 2.03–2.15 (m, 4H), 2.82 (brs, 1H), 2.94–3.16 (m, 13H), 3.46–3.51 (m, 2H), 3.57 (brm, 1H), 3.67–3.77 (m, 3H), 4.14 (brm, 1H), 4.19–4.27 (m, 2H), 4.37 (brm, 1H), 5.14 (brm, 1H), 5.31 (brm, 1H), 6.18 (brm, 1H), 6.58 (d, *J* = 9.0 Hz, 1H), 7.11–7.24 (m, 10H); ¹³C NMR (100 MHz, CDCl₃) δ 27.8, 28.0, 37.7, 38.1, 38.77, 38.79, 38.84, 41.8, 52.8, 52.9, 53.0, 53.1, 55.4, 55.9, 66.79, 66.84, 69.4, 69.6, 69.7, 69.9, 79.8, 126.5, 126.6, 128.4, 128.4, 129.0, 129.2, 155.1, 170.6, 170.9; HRMS-FAB (M + Na⁺) calcd for C₂₁H₃₀N₂NaO₄S₂ 461.1545, found 461.1544.

(Methoxysuccinyl) tetrahydropyranone 28. A solution of **24** (200 mg, 0.46 mmol) and TFA (3 mL) in CH₂Cl₂ (7 mL) was stirred at 25 °C for 1 h. This solution was concentrated, and the resulting material was triturated with ether to precipitate the TFA salt as a white solid. This solid was washed with ether, dried under vacuum, and then added to a solution of methyl succinate (61 mg, 0.46 mmol), 1-hydroxybenzotriazole (HOBT, 72 mg, 0.46 mmol), 1-(3-(dimethylamino)propyl)-3-ethylcarbodiimide hydrochloride (EDC, 114 mg, 0.60 mmol), and *N*-methylmorpholine (0.10 mL) in CH₂Cl₂ (5 mL). The reaction was stirred overnight at room temperature, and then it was washed with water, 1 M KHSO₄, saturated Na₂CO₃, and dried over Na₂CO₃. The dried solution was concentrated, and the crude material was purified by flash chromatography (7:3 EtOAc/hexanes) to yield a mixture of diastereomers of **28** (144 mg, 70%) as a white solid: ¹H NMR (400 MHz, CDCl₃) δ 2.11–2.14 (m, 4H), 2.45–2.50 (m, 2H), 2.52–2.54 (m, 2H), 2.57–2.64 (m, 4H), 2.97–3.13 (m, 5H), 3.19–3.26 (m, 9H), 3.53–3.62 (m, 3H), 3.65 (s, 3H), 3.67 (s, 3H), 3.76–3.86 (m, 3H), 4.17–4.22 (m, 1H), 4.26–4.31 (m, 1H), 4.66–4.71 (m, 1H), 4.77–4.82 (m, 2H), 6.25 (d, *J* = 6.3 Hz, 1H), 6.68 (d, *J* = 9.1 Hz, 1H), 6.77 (d, *J* = 8.0 Hz, 1H), 6.96 (d, *J* = 7.7 Hz, 1H), 7.21–7.30 (m, 10H); ¹³C NMR (100 MHz, CDCl₃) δ 29.0, 29.1, 30.59, 30.61, 37.9, 38.2, 38.81, 38.88, 38.93, 41.9, 51.6, 53.0, 53.3, 54.3, 54.7, 66.9, 67.0, 69.48, 69.50, 69.7, 69.9, 126.6, 126.8, 128.4, 128.5, 129.1, 129.3, 136.5, 170.3,

170.7, 171.2, 171.4, 172.9, 173.0; HRMS-FAB ($M + Na^+$) calcd for $C_{21}H_{28}N_2NaO_5S_2$ 475.1338, found 475.1349.

Tetrahydropyranone Inhibitors 32a and 32b. A solution of *N*-bromosuccinimide (NBS, 440 mg, 2.47 mmol) in 80% aqueous MeCN (10 mL) was cooled in an ice bath. To this solution was added **28** (160 mg, 0.35 mmol) in MeCN (5 mL). The ice bath was removed, and the reaction mixture was stirred for 10 min. It was then partitioned between 1:1 CH_2Cl_2 /EtOAc (25 mL) and saturated Na_2SO_3 (10 mL). The organic layer was separated, washed with saturated $NaHCO_3$ and brine, and dried over Na_2CO_3 . The dried solution was concentrated, and the residue was redissolved in 1:1 MeCN/ H_2O . This solution was filtered and extracted with 1:1 CH_2Cl_2 /EtOAc. The resulting organic layer was dried and concentrated to yield a mixture of diastereomers of **32** (88 mg, 66%) as a white solid. The diastereomers were separated by HPLC (silica) with 3.5% 2-propanol in CH_2Cl_2 as the mobile phase. The retention times for diastereomers **32a** and **32b** were 13.1 and 14.1 min, respectively. For **32a**: 1H NMR (400 MHz, $CDCl_3$) δ 2.45–2.48 (m, 3H), 2.59–2.74 (m, 3H), 2.93 (t, $J = 9.9$ Hz, 1H), 3.03 (m, 1H), 3.12–3.14 (m, 1H), 3.55 (t, $J = 11.4$ Hz, 1H), 3.67 (s, 3H), 4.29 (brm, 1H), 4.42 (brm, 1H), 4.61 (brm, 1H), 4.72 (brm, 1H), 6.28 (brm, 1H), 6.59 (brm, 1H), 7.17–7.31 (m, 5H); ^{13}C NMR (100 MHz, $CDCl_3$) δ 29.1, 30.9, 38.3, 42.2, 51.9, 54.4, 57.3, 68.8, 71.6, 127.1, 128.7, 129.2, 136.3, 170.7, 171.3, 173.4, 202.5; HRMS-FAB ($M + Na^+$) calcd for $C_{19}H_{24}N_2NaO_6$ 399.1532, found 399.1537. For **32b**: 1H NMR (400 MHz, $CDCl_3$) δ 2.45–2.48 (m, 3H), 2.59–2.78 (m, 3H), 3.02–3.06 (m, 1H), 3.10–3.13 (m, 2H), 3.59 (t, $J = 11.5$ Hz, 1H), 3.67 (s, 3H), 4.27–4.32 (m, 1H), 4.54 (m, 2H), 4.73 (brm, 1H), 6.32 (brm, 1H), 6.66 (brm, 1H), 7.17–7.31 (m, 5H); ^{13}C NMR (100 MHz, $CDCl_3$) δ 29.1, 30.9, 38.2, 42.1, 51.8, 54.3, 57.5, 68.8, 71.8, 127.1, 128.7, 129.2, 136.1, 170.9, 171.3, 173.3, 202.2; HRMS-FAB ($M + Na^+$) calcd for $C_{19}H_{24}N_2NaO_6$ 399.1532, found 399.1521.

Measurement of K_{H_2O} and K_{RSH} by 1H NMR Spectroscopy. These equilibrium constants were measured at 25 °C on a Bruker AM-400 NMR spectrometer according to the procedures of Burkey and Fahey.^{18,23} Cyclohexanone, tetrahydropyran-4-one, tetrahydrothiopyran-4-one, and 4-piperidone hydrochloride were purchased from Aldrich Chemical Co. and used without further purification. NMR samples were prepared by dissolving the ketone (100 mM) in D_2O . For measurements of K_{RSH} , the concentration of 3-mercaptopyruvic acid was 200 mM.

Racemization of Inhibitors. The racemization of the cyclohexanone inhibitors **30a** and **30b** was followed by RPHPLC using the conditions reported above for the separation of the two diastereomers. Each diastereomer was dissolved in 100 mM phosphate buffer at pH 6.5. Less than 5% racemization was detected after 24 h.

The racemization of the tetrahydropyranone inhibitors **32a** and **32b** was monitored using 1H NMR spectroscopy by integration of the methyl ester signal at 3.47 ppm for **32a** and 3.45 ppm for **32b**. Each diastereomer was dissolved in 100 mM phosphate buffer at pH 6.5 that was prepared using D_2O . The observed first-order rate constant for racemization was measured to be $k_{obsd} = (2.2 \pm 0.5) \times 10^{-3} \text{ min}^{-1}$. This rate constant corresponds to a half-time for racemization of 5.25 h. Thus, over the time period of a typical enzyme assay, less than 1% of each diastereomer of the inhibitor will have racemized to the undesired diastereomer.

Racemization experiments for the piperidone-based inhibitor were performed using compounds **35a** and **35b**. These diastereomers were separated by HPLC with an eluent of 2% MeOH in CH_2Cl_2 (**35a** retention time 15.5 min; **35b** retention time 20.5 min). The Cbz protecting group in each diastereomer was removed using the procedure reported for the preparation of compound **34**, which yielded compounds **36a** and **36b**. 1H NMR spectra demonstrated that these deprotections occurred with retention of stereochemistry. Diastereomer **36a** was split into two samples and each placed in an NMR tube. One sample was dissolved in 100 mM phosphate buffer (pH 6.5) that was prepared using D_2O . The 1H NMR spectrum of this sample demonstrated that the compound was completely racemized within 10 min under these conditions. The second sample was dissolved in 1:1 acetone- d_6 / D_2O . 1H NMR of this sample showed relatively slow reaction, with complete racemization after approximately 22 h. Diastereomer **36b** gave similar

results. For **36a**: 1H NMR (400 MHz, $CDCl_3$) δ 1.98 (brs, 3H), 2.45–2.54 (brm, 3H), 3.06 (brs, 1H), 4.38–4.45 (brm, 2H), 4.75–4.82 (brm, 2H), 5.17 (brm, 2H), 6.34 (brs, 1H), 6.79 (brs, 1H), 7.18–7.38 (brm, 10H); ^{13}C NMR (100 MHz, $CDCl_3$) δ 23.2, 38.5, 40.4, 44.1, 48.7, 54.4, 56.6, 67.9, 127.1, 128.0, 128.2, 128.6, 128.7, 129.2, 136.2, 154.8, 170.0, 171.1, 202.88, 202.94; HRMS-FAB ($M + Na^+$) calcd for $C_{24}H_{27}N_3NaO_5$ 460.1849, found 460.1860. For **36b**: 1H NMR (400 MHz, $CDCl_3$) δ 1.98 (brs, 3H), 2.44 (brm, 3H), 3.01 (brm, 3H), 4.46 (brs, 2H), 4.67–4.76 (brm, 2H), 5.18 (brm, 2H), 6.38 (brs, 1H), 6.68 (brs, 1H), 7.19–7.40 (brm, 10H); ^{13}C NMR (100 MHz, $CDCl_3$) δ 23.2, 38.7, 40.4, 44.2, 48.5, 54.5, 56.3, 67.9, 127.0, 128.0, 128.3, 128.6, 128.7, 129.3, 136.2, 136.4, 154.8, 170.2, 170.9, 203.2; HRMS-FAB ($M + Na^+$) calcd for $C_{24}H_{27}N_3NaO_5$ 460.1849, found 460.1849.

Papain Assays. Papain (recrystallized two times) and L-BAPNA (*N* α -benzoyl-L-arginine *p*-nitroanilide hydrochloride) were used as received from Sigma Chemical Co. Reaction progress was monitored with a Perkin-Elmer 8452A diode array UV-vis spectrometer. Papain was assayed at 25 °C in 100 mM phosphate buffer (pH 6.5) containing 5 mM EDTA and 5 mM cysteine. BAPNA and inhibitor stock solutions contained DMSO (10–100%), and all assay mixtures contained a final DMSO concentration of 10%. Papain stock solutions (0.5–1 mg/mL) were prepared in buffer (5 \times), and the enzyme was activated for 1 h before the assays were run. Initial rates were determined by monitoring the change in absorbance at 412 nm from 60 to 120 s after mixing. None of the inhibitors showed evidence of slow binding. The more potent diastereomer of each inhibitor was subjected to full kinetic analysis. For each inhibitor concentration examined (**30a** 0, 21, 53, 107, 160, 217 μ M; **31a** 0, 2.7, 5.5, 27.4, 55, 110 μ M; **32a** 0, 2, 25, 50, 75, 100 μ M; **34a** 0, 13.9, 69.5, 139, 209, 417 μ M) at least five substrate concentrations were used (**30a** 0.37, 0.53, 0.75, 1.5, 7.5 mM; **31a** 0.5, 0.66, 0.99, 2.0, 6.6 mM; **32a** 0.5, 0.65, 0.94, 1.7, 4.5, 8.0 mM; **34a** 0.5, 0.66, 0.99, 2.0, 6.6 mM) with at least two independent determinations at each concentration. K_m was measured to be 4.89 mM. The background hydrolysis rate was less than 1% of the slowest rate measure and thus ignored. K_i values were determined by nonlinear fit to the Michaelis–Menten equation for competitive inhibition using simple weighing. Competitive inhibition was confirmed by Lineweaver–Burk analysis using robust statistical weighing to the linear fit of $1/[V]$ vs $1/[S]$. For the less-potent diastereomer of each inhibitor, a single substrate concentration (**30a** 5.28 mM; **31a** 3.30 mM; **32a** 4.22 mM) was monitored at with least 4 different inhibitor concentration (**30a** 0, 130, 410, 830 μ M; **31a** 0, 0.14, 0.29, 0.57, 1.14, 1.72 mM; **32a** 0, 0.1, 0.56, 1.1, 1.5, 1.9 mM). Competitive inhibition was assumed, and K_i was calculated using a Dixon analysis. Data analysis was performed with the commercial graphing package Grafit (Erithacus Software Ltd).

Acknowledgment. This research was supported by the American Cancer Society (grant IN-45-36), the American Chemical Society–Petroleum Research Fund (grant 30544-G4), the U.S. Army Medical Research and Materiel Command–Breast Cancer Research Initiative (Career Development Award to C.T.S., grant DAMD17-96-1-6328), and Brown University (Salomon Faculty Research Award). T.C.S. was supported by a Department of Education GAANN Fellowship and by the USAMRMC–Breast Cancer Research Initiative (Predoctoral Fellowship, grant DAMD17-96-1-6037). J.L.C. was supported by a GAANN Fellowship and by a University Fellowship from Brown University. We thank Professor David Cane for use of his UV-vis spectrometer.

Supporting Information Available: Lineweaver–Burk plots for the inhibition of papain by compounds **30**–**32** and **34**; 1H and ^{13}C NMR characterization for compounds reported in the Experimental Section; experimental details of the synthesis of inhibitors **30**, **31**, and **34** (55 pages). See any current masthead page for ordering and Internet access instructions.